Future Circular Collider

PUBLICATION

Analysis of vacuum stability at cryogenic temperature: Deliverable D4.1

Cimino, Roberto (INFN e Laboratori Nazionali di Frascati (IT))
et al.

30 January 2019

The European Circular Energy-Frontier Collider Study (EuroCirCol) project has received funding from the European Union's Horizon 2020 research and innovation programme under grant No 654305. The information herein only reflects the views of its authors and the European Commission is not responsible for any use that may be made of the information.

The research leading to this document is part of the Future Circular Collider Study

The electronic version of this FCC Publication is available on the CERN Document Server at the following URL :
<http://cds.cern.ch/record/2655290>

Grant Agreement No: 654305

EuroCirCol

European Circular Energy-Frontier Collider Study

Horizon 2020 Research and Innovation Framework Programme, Research and Innovation Action

DELIVERABLE REPORT

ANALYSIS OF VACUUM STABILITY AT CRYOGENIC TEMPERATURE

Document identifier:	EuroCirCol-P2-WP4-D4.1
Due date:	End of Month 22 (April 1, 2017)
Report release date:	31/03/2017
Work package:	WP4 (cryogenic beam vacuum system)
Lead beneficiary:	ALBA
Document status:	RELEASED (V1.0)

Abstract:

Vacuum stability at cryogenic temperature is a key element for the design of the proton-proton future circular collider FCC-hh. To thermally screen the cold bore of all superconducting magnets a beam screen is a mandatory solution. Its design, operating temperature and structure must fulfil a number of different technical requirements. Other groups, within the EuroCirCol collaboration, are producing design studies and prototypes to be validated as base line beam screen for the final study objective of the collaboration. Among such requirements, vacuum stability at cryogenic temperature is indeed a very important one, being the object of the present report.

The objective of the task 4.4, within the WP4, is to validate on small test samples, the proposed temperature and the various material surfaces produced by the collaboration. This task will be honored by using two dedicated UHV systems to study gas adsorbion/desorbtion on small test samples as indicated/produced by the others members of the collaboration.

The ongoing activity to characterise the available systems and to set up an experimental strategy to study such test samples, once available, will be here presented. Secondary Electron Yield (SEY) has been individuated as a novel technique to be associated to Temperature Programmed Desorption (TPD) and mass spectrometry to qualify beam screen materials and their adsorption/desorption properties.

The European Circular Energy-Frontier Collider Study (EuroCirCol) project has received funding from the European Union's Horizon 2020 research and innovation programme under grant No 654305. EuroCirCol began in June 2015 and will run for 4 years. The information herein only reflects the views of its authors and the European Commission is not responsible for any use that may be made of the information.

Delivery Slip

	Name	Partner	Date
Authored by	Roberto Cimino Marco Angelucci Francis Perez Paolo Chiggiato	INFN INFN ALBA CERN	10/03/17
Edited by	Julie Hadre Johannes Gutleber	CERN	16/03/17
Reviewed by	Michael Benedikt Daniel Schulte	CERN	22/03/17
Approved by	EuroCirCol Coordination Committee		31/03/17

TABLE OF CONTENTS

1. INTRODUCTION

Vacuum stability at cryogenic temperature is a key element for designing and careful choosing materials to be used in the construction of the highest Energy Proton machine FCC-hh.

The cold bore of all superconducting magnets must not see any Synchrotron radiation nor any heat load sources associated with the circulating beam to avoid unbearable heat load transfer onto it. Therefore, a beam screen (like in LHC) is a mandatory solution to intercept all those heat sources and dissipate them at higher temperatures than the cold bore. The actual shape, the material choice and the operating temperature of such a beam-screen, must be chosen provided that a number of different technical requirements are respected. Other groups, within the EuroCirCol collaboration, are producing design studies and prototypes to be validated in order to define the proposed base line beam screen in the design study objective of the collaboration. Among such requirements, vacuum stability at cryogenic temperature is indeed a very important one.

The beam screen temperature will be chosen according to different (and sometimes) contradictory requirements. In simple terms, the beam screen need to be held at as low as possible cryogenic temperatures to reduce thermal radiation to the cold bore, and to limit the machine impedance budget. It is well known that metals, at low temperatures, have a lower resistivity than at room temperatures. This will directly correspond to a reduced impedance if the BS will be working at as low as possible temperatures. The importance of minimizing the machine impedance budget is a very serious issue. So much that other groups are studying the possibility of depositing HTc superconductors as inner BS material to enhance its surface conductivity. In that case, of course, the BS temperature must be at least below the superconductor critical temperature. If one consider, as for the LHC beam screen, and internal surface of Cu, impedance consideration suggests to operate the BS below at least 60K.

On the other hand, the lower the BS temperature, the highest the complexity and cost of the beam screen cooling system will be, since it will have to deal with the severe heat load deposited by Synchrotron radiation of more than 30 W/m (about a factor 100 more than for the LHC). The complexity and cost to remove any heat load from a surface is inversely proportional to its base temperature. First estimates suggest that it may become unfeasible to design a beam screen to be held at or below 20 K, as it is now for LHC.

To decide the best temperature window at which one should design and operate the beam screen for FCC-hh, one must find the right compromise between those aforementioned items and the required BS vacuum stability. In simple terms, given the notion that the beam screen temperature may vary, during operation, by few degrees, the chosen temperature has to be such that either a gas is always cryosorbed in a stable manner onto it or always not, in the entire temperature range foreseen.

If the temperature chosen is such that a small unavoidable temperature fluctuation induces complete gas desorption of an otherwise cryosorbed layer, this may cause pressure burst and a severe malfunction of the machine. This issue is better understood by looking at Figure 1, were saturated vapour pressures are shown for different gasses. Each line, following the Clausius-Clapeyron equation, shows the pressure and temperature at which a thick layer of adsorbed gas can coexist with its vapour. This plot is extremely instructive. For FCC-hh, lifetime and radiation consideration require that the base total pressure in the dipoles should range between 10^{-10}- 10^{-12} mbar. Those extremely low pressure can be achieved due to the fact that the cold bore at 1.9 K is an extremely powerful pump acting on the vacuum vessel trough opportunely designed pumping slots.

Residual gasses in the vacuum system may come from atmosphere and are typically formed by: H_2, CO, CO_2, CO, CH_4, H_2O, Ar, and their partial pressure will depend on many aspects being always below 10^{-10}- 10^{-12} mbar.

For LHC the beam screen temperature window was chosen to be between 5 K and 20 K. In this region, as from Figure 1, gasses are either stably adsorbed on the BS surface or free to diffuse to the cold bore surface, which is acting as a very efficient gas sink in the LHC. From Figure 1, a temperature between 40 K and 60 K and one between 90 and 110 K have been individuated to allow vacuum stability of thick ices. The 90–110 K region should be excluded for impedance reason while the 40 -60 K one needs to be studied in details.

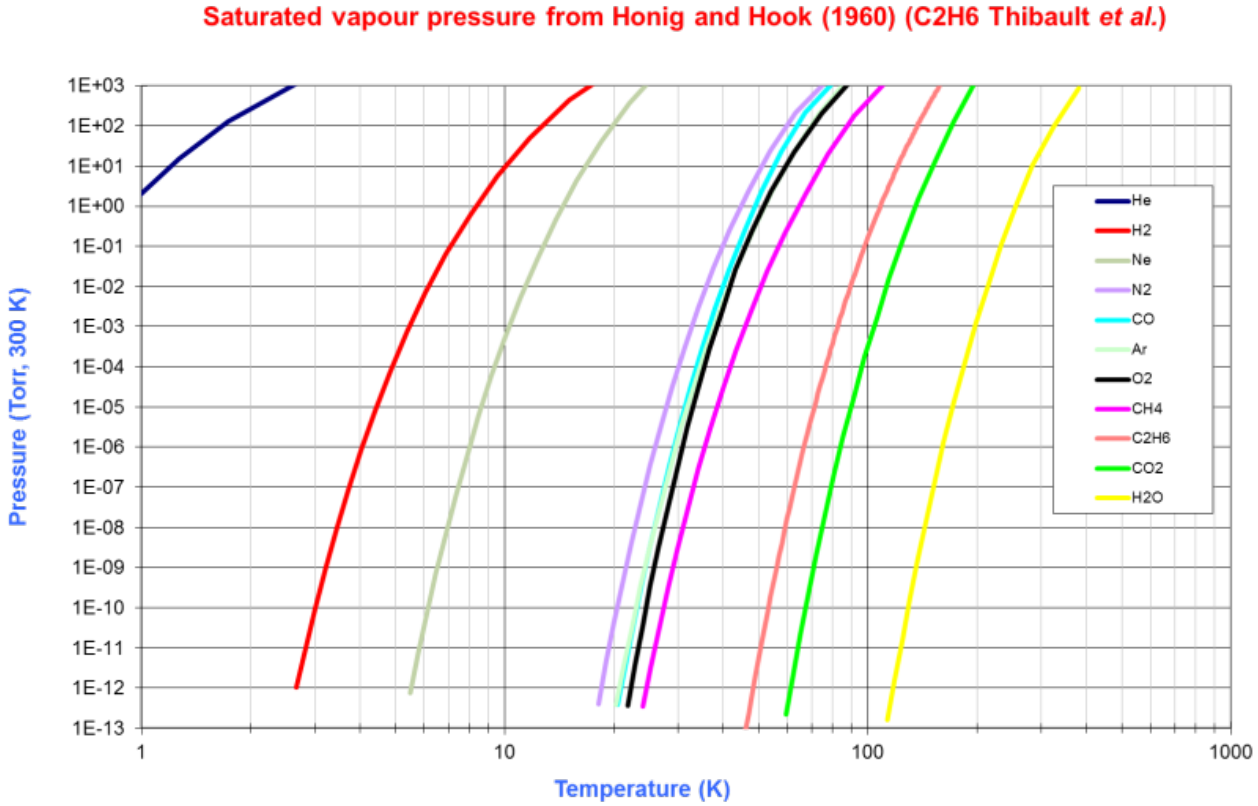

Figure 1: Saturated vapour pressure from Honig and Hook (1960) (C2H6 from Thilbault et al.)

As said, Figure 1 is valid for thick ices, for smooth surfaces and in absence of any non-thermal desorption mechanisms. In FCC-hh, surfaces may not be very smooth, sub to few monolayer coverage may be important, and indeed, the surface will be irradiated by photons, electrons and ions, which definitely will induce non-thermal desorption that need to be studied in great details.

One more issue, to be considered in this context, is that for beam instability reasons, not discussed here, detrimental electron cloud may form in the vacuum system depending on the Secondary Electron Yield (SEY) of the exposed surface. For this reason, different proposed materials are analysed in other tasks of our WP by O. Malyshev et al, to find the best coating material to mitigate this issue. One proposed solution is to use laser treated Cu surfaces to geometrically reduce Cu SEY to safe values. If this proposal seems to be excellent as an electron cloud mitigator, it will introduce macroscopically and microscopically rough surfaces inside the vacuum system. It is well known that rough surfaces geometrically increase the surface available for gas to condensate, rendering them like sponges. Such modified surfaces can host much more cryosorbed gases per adsorbed monolayer than their flat counterparts so that the low coverage regime (few monolayers) may become extremely important and to be studied in details. At low coverages, it is in fact well known that the adsorbed ice does interact

with the substrate and can modify the otherwise universal saturated vapour pressure curves of Figure 1.

Moreover, gas adsorption on cold surfaces (being flat or macro-microscopically rough) will anyway influence and modify their SEY, that is their ability to mitigate detrimental electron cloud issues, and this effect must be analysed carefully. As shown in Figure 2, after a certain ice thickness of condensed gas the SEY max will be only determined by the gas species cryosorbed on the surface, independently from the original SEY max of the substrate. For the case of laser treated surfaces, we still expect efficient SEY max reduction due to the surface geometry, but the final SEY value of interest to the machine stability will be also determined by the gas adsorbed and /or trapped in the microstructures, so this issue has to be taken into account and need to be studied in details.

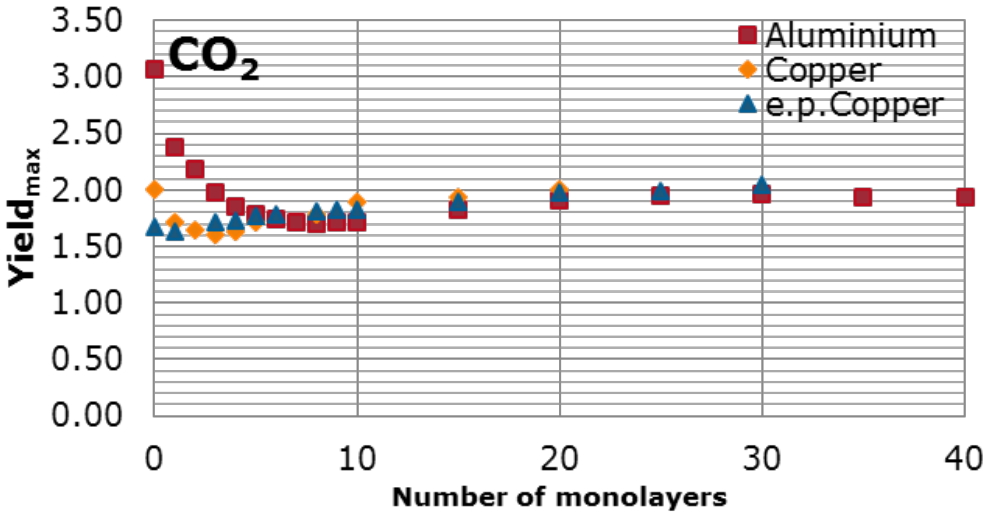

Figure 2: maximum of SEY versus CO_2 coverage on cold surfaces. [1]

This, in simple terms, is the scientific challenges of our WP, and its different tasks, has to face. At LNF – INFN we are going to contribute to some of the aforementioned scientific aspects by using two experimental set ups that will be presented in the next section, to study gas adsorbion/desorbtion on small test samples, once available from the collaboration. Clearly all issues on vacuum stability can not be solved by a single laboratory and a collaborative, multidiscipline and international effort has to be coordinated to finalize this study.

2. DESCRIPTION OF THE EXPERIMENTAL APPARATA AVAILABLE AT LNF

The laboratory in use for contributing to the study object of this collaboration, essentially consists of two UHV experimental systems used in past years to contribute to study material properties of interest to accelerators [2-10]. With those two systems, we were able to measure and address the importance of low energy electrons in SEY, being one of the few laboratory in the word able to measure SEY from work function landing energy onwards, both at RT and at LT [2-7]. With the available system, we were able to individuate the chemical origin of "scrubbing" the electron cloud mitigation strategy adopted at LHC by simultaneously measure SEY and XPS [2, 8-10]. Those set ups, have been dedicated to SEY study and are now upgraded to study vacuum stability. As the description of the recent activities will clarify, we are in a position to use and qualify SEY, not only as a technique to study essential parameters for instabilities simulation, but also as an investigation tool to study thermal desorption in presence of an electron flux. This seemingly unique feature is now available to the collaboration and we are confident that it will contribute to the final understanding of most aspects involved in determining design and material choice to cope with the stringent requirements granting vacuum stability.

During the course of the EuroCirCol project INFN is supporting the project with extra funding to update the experimental stations here described: both stations will be equipped with a close cycle He cryostat to operate at temperatures of interest (from 15 K to 300 k) and with a state of the art mass spectrometer.

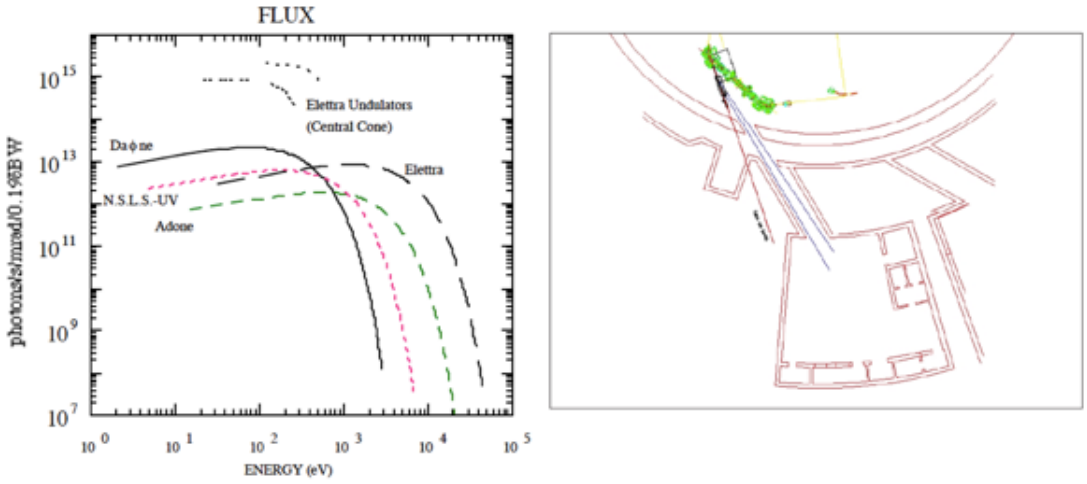

Figure 3: (Left Panel): Total flux emitted in the vertical plane (per horizontal mrad) by the bending magnets of DAΦNE and of other SR. (Right Panel): The SR DAΦNE bending magnet and the existing laboratory

The two setups available at LNF-INFN to this project have been designed to be used as stand-alone systems but also as end stations of two corresponding beamlines (at present under commissioning). This will enable us to have access to the Synchrotron Radiation as emitted by a bending magnet from DAΦNE, the running 500 MeV accelerator, presently operating in Frascati. The Synchrotron radiation spectrum emitted by DAΦNE is shown in Figure 3(left panel) while the laboratory building with the two beamlines is schematically shown of Figure 3 (right panel). One beamline, named XUV1, will cover the energy range between 60-1000 eV. The expected resolving power is ranging between 500 to 5000 with a photon flux ranging from 10^{10} to 10^{12} ph/ s/1%bw in the entire energy range. The spot size

on the sample will depend on various settings but can be estimated to be about 1 mm^2. At the end of this beamline the XUV1 end station will be mounted. A second beamline, named XUV2, will cover the energy range between 35-150 eV. The expected resolving power is ranging between 200 to 5000 with a photon flux ranging from 10^{10} to 10^{12} ph/ s/1%bw in the entire energy range. The spot size on the sample will be ~ 1 mm^2. At the end of this beamline the XUV2 end station will be mounted.

It is here worth mentioning that, we are presently considering to partially utilize the laboratory, to exploit SR at DAΦNE to study in detail reflectivity, photo-yield and photo induced desorption. A Memorandum of Understanding (MoU) with CERN is getting finalized and, in this context, it is conceivable to deviate the white light entering the laboratory, in a dedicated beamline to irradiate long (up to 2-3 meters) samples. This new set-up will allow us to obtain complementary data to the ones obtainable on small surface samples from the other two beamlines.

At present, the two end stations are used as stand-alone setups for surface science studies. In the next months, the presence of monochromatic photons in the range between 35 eV to 1000 eV will become available for additional studies on photo desorption from small samples.

2.1. XUV1 END STATION

The XUV1 end station is a “state of the art” ultra-high-vacuum system for XPS, UPS, Secondary Emission Yield (SEY) and LEED surface spectroscopy.

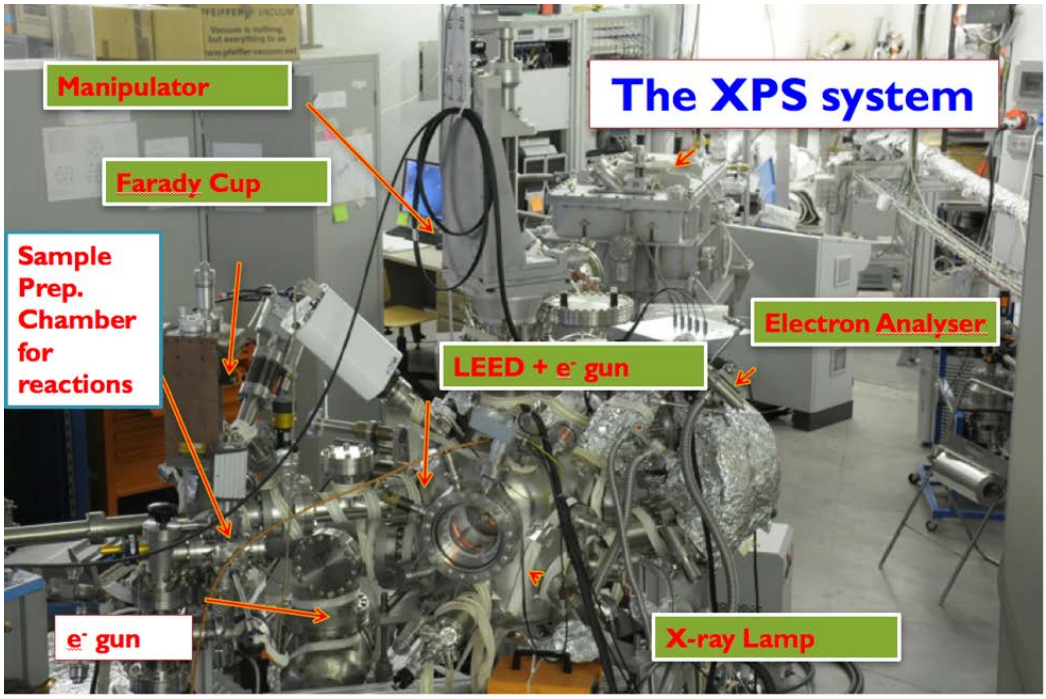

Figure 4: Picture of XUV1 experimental station.

The system, shown in Figure 4, is composed by a main analysis chamber connected to a preparation chamber by means of a gate valve. The system is equipped with a fast entry lock and a sample transfer mechanism which allow to insert the sample in UHV without breaking the vacuum. In the preparation chamber, the sample can be Ar^+ sputtered, heated to high-T by means of electron bombardment or by a Boron-Nitride heating element and exposed to various gases. At the end of the present year this chamber will be implemented with a low temperature manipulator and a state-of-the-art quadrupole mass spectrometer, to be able to perform XPS, TPD SEY and all other studies on the LT surfaces of interest to this study.

2.2. XUV2 END STATION

The XUV2 end station is already equipped with a LT close cycle manipulator and is the system used to collect all data presented in the following section. It consists of a μ-metal ultra- high-vacuum system for Angle Resolved UV Spectroscopy (ARUPS) and SEY.

This second UHV system, shown in Figure 5, shares with the previous one the structure based on the preparation chamber, the analysis chamber and a fast entry lock facility as well as the possibility to clean and heat the sample and to grow thin films on small area substrates. The peculiar characteristics of this system consist in the possibility to perform ARUPS and to measure SEY-curves. A monochromatic, small-spot UV source is available in the analysis chamber, where the sample under study can be cooled down to 15 K by a close cycle refrigerator. At the end of the present year this chamber will be implemented with a state–of-the-art quadrupole mass spectrometer, to be able to perform LT SEY TPD, ARUPS and all other studies on the surfaces of interest to this project.

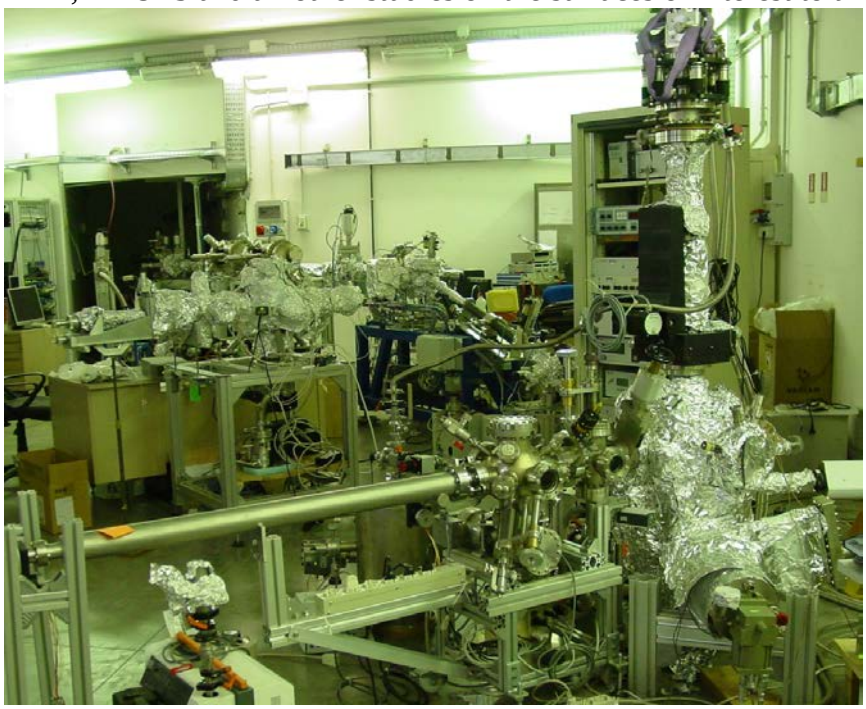

Figure 5: Picture of XUV2 experimental station

3. DESCRIPTION OF EXPERIMENTAL ACTIVITY PERFORMED.

To test the available system, we performed preliminary studies following the SEY behaviour during the adsorption and desorption of Ar and CO on a clean polycrystalline Cu surface at cryogenic temperature. The adsorption and desorption process of these gases could give a significant pressure variation induced by temperature oscillation around 20 K, as discussed above (Figure 1). For this reason, an accurate study of these phenomena is chosen as starting point to investigate new systems and to understand the effect of electron beam. The clean polycrystalline Cu substrate was chosen since it has a stable SEY during electron bombardment [6, 9].

We performed measurements following the effect of the adsorbate layer thickness on the number of secondary electrons emerging from a cold surface. Primary electrons can be elastically reflected or generate secondary electrons. These two effects have different weight as depending on the detailed properties of the system and its surface [2, 3]. Generally speaking, it is assumed [2, 4] that for primary energy (Ep) <50 eV the contribution of reflected electrons to SEY might become relevant, whereas the contribution of secondary electrons might be negligible. On the contrary for Ep>50 eV the contribution of reflected electrons is negligible and SEY curve is dominated by the secondary emission. Particular attention was paid to the first region since SEY measured for primary energy below 50 eV can give additional information on low adsorption gas coverage.

The experiments were performed in an Ultra-High Vacuum (UHV) system, with a base pressure better than $2 \cdot 10^{-10}$ mbar. The main chamber is equipped with a low temperature manipulator that can reach a temperature of 10 K thanks to a helium close cycle cooling system. An 8 mm square polycrystalline Cu substrate was mounted on a copper sample-holder in order to maximise the thermal and electrical conductivity with the manipulator. The Cu substrate was cleaned with cycles of Argon sputtering of 1 h at 750 eV until a SEY curve similar to that reported in literature was observed. The SEY data were acquired at different steps as a function of/to the exposure that is reported in Langmuir (L). ($1\ \mathrm{L} = 10^{-6}$ torr s)

The Secondary Electron Yield is defined as:

$$SEY\ (Ep) = Iout\ /Ip = (Ip - Is)\ /\ Ip = 1 - (Is\ /\ Ip)$$

where *Ep* and *Ip* are respectively the energy and the current of the primary electrons, *Iout* is the current of the secondary emitted electrons and *Is* is the sample current to ground. In order to obtain an accurate measure of the SEY at primary energy close to zero, the primary current was measured through a Faraday cup. The primary electrons are generated by an electron gun in a Ep range between 5 and 1000 eV. The SEY measurements were performed at normal incidence. More details of the used system can be found in literature [2-10].

Controlled gas quantities were introduced in the UHV chamber through a leak valve. During the exposure, the pressure was maintained constant at $2 \cdot 10^{-8}$ mbar. In order to induce minimal interaction between primary beam and adsorbates during data acquisition, an electron beam current of a few nA was used.

The gas desorption was measured heating the sample from 10 to 100 K by a resistive heater, with a rate of 1.7 K/min. In order to obtain a SEY measure at constant temperature, with an error less than 1 K, during the heating procedure a fast scan, with a total scan time less than 30 seconds, was used. It is worth mentioning here, that we have an open geometry which grants the fact that there is no (or very little) gas re-adsorption on the surface during desorption, so that, TPD result are expected to be accurate.

3.1. ARGON ICES

Figure 6a shows the SEY curves measured at 10 K on the surface of a clean polycrystalline copper sample before and after the exposure to increasing quantities of Ar atoms. The SEY curves measured with high-energy resolution in the range between 0 to 90 eV are reported in Figure 6b. Both figures show also the SEY curves measured on clean copper at RT (black lines) that presents the characteristic features between 0 and 60 eV with a minimum of 0.07 at 10 eV, and a maximum of 1.4 at Ep> 550 [9]. For the clean metal, the spectrum measured at 10 K presents slight modifications in the low energy range where the minimum value changes to 0.35. These changes are not intrinsic to temperature variation but are due to sub monolayer (ML) contamination during sample cooling down. In more controlled runs, in fact, SEY and LE-SEY of Cu measured at RT and LT are essentially identical.

For the Ar exposed copper, SEY curves show new features as a function of dose. It is useful to identify different dosing steps. During the first steps, significant variations in the low-energy range are observed and SEY increases up to 0.5 at Ep=10 eV. Furthermore, a slight increase up to 1.4-1.5 is observed also for Ep>500 eV. This can be ascribed to the adsorption of the first ML after an Ar dose of 7 L SEY increases up to 0.65 and 1.6 in the low and high-energy region respectively. For higher Ar doses, SEY does not significantly change at Ep=10eV and presents a progressive increase up to 3.9 at Ep ~700 eV.

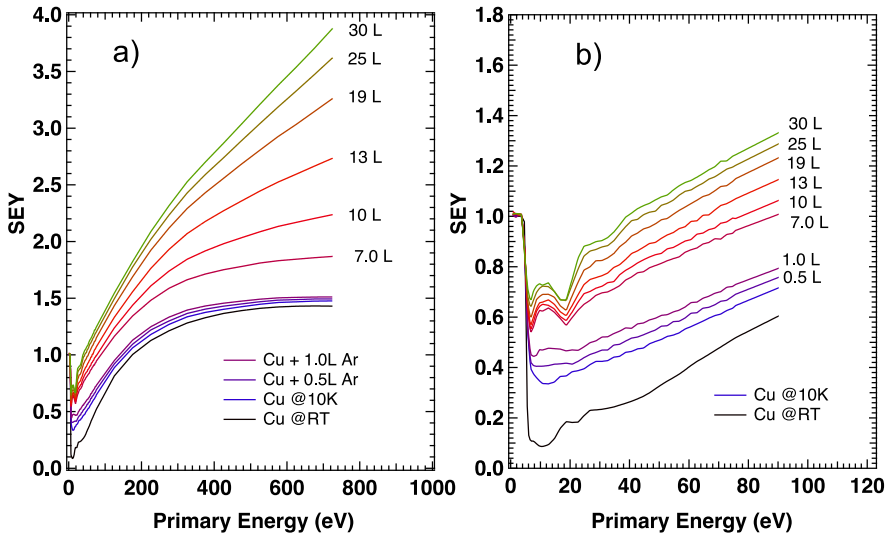

Figure 6: SEY curves versus primary electrons energy as function of Ar dose. In the left panel (a) it is shown the behaviour in the complete region between 0 and 720 eV. In the right panel (b) it is presented an enlargement of the region between 0 and 90 eV

Figure 7a shows the SEY behaviour at Ep=10 and 720 eV as a function of the Ar dose. Ep=10 eV is chosen to follow the evolution of SEY at Low-landing Energy of the Primary Beam (LEPB), while

Ep=720 eV is chosen for High-landing Energy (HEPB). Different trends are observed in the two energy regions as a function of the adsorption of progressively thicker Ar layers on the Cu sample.

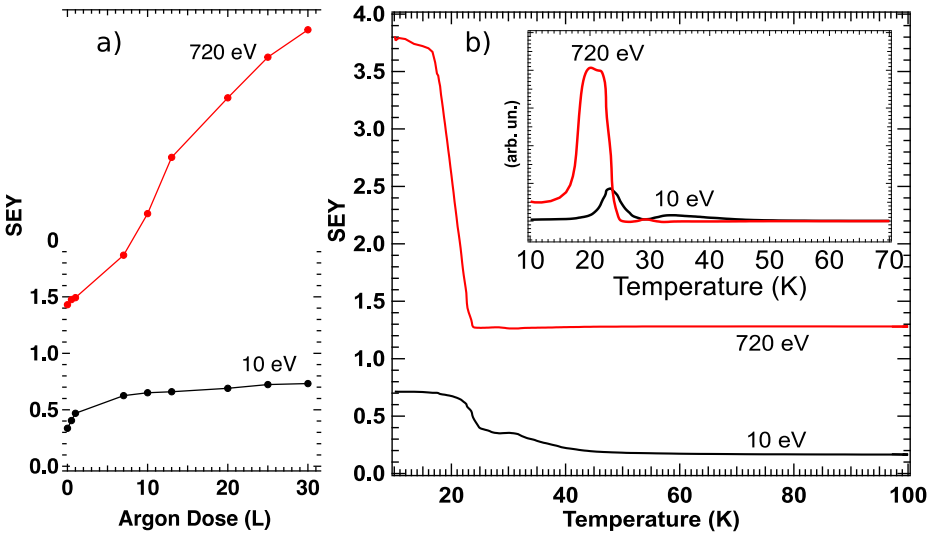

Figure 7: SEY trend versus argon dose (left panel) and versus temperature (right panel) at specific primary energies. (Right panel insert) First derivatives of SEY curves versus temperature.

In particular, with the first exposure steps, the formation of an Ar single layer on the surface, interacting with primary electrons, introduces significant SEY variations in LEPB range but does not influence electrons in the HEPB region. As already discussed [3], it is possible to correlate the SEY in LEPB and HEPB regions with reflected and emitted secondary electrons respectively; because of this, it is reasonable to attribute the modifications in the LEPB range to a variation in the total electron reflectivity of the surface. On the contrary, the formation of an Ar multilayer changes significantly also the interaction with high-energy primary electrons, generating a large number of secondary electrons and consequently a strong, and continuous, increase in SEY is visible. This is in good agreement with literature [11]. It has been observed that when a very high quantity of gas is adsorbed on the substrate, the primary electrons interact only with Ar ice and SEY becomes constant [11]. For very thick multilayers, the Ar ice becomes insulating, charges up and it is not possible, with our actual system, to measure SEY. For this technical reason, the dosing process was stopped at 30 L.

The Cu sample with the Ar multilayer on top was heated up to 100 K. The evolution of SEY at Ep=10 and 720 eV as a function of temperature is shown in Figure 7b. For a better evaluation of the desorption temperature the curves in Figure 7b have been differentiated and the results are shown in the inset of Figure 7b. The curve at Ep=720 eV, during the desorption process of Ar, presents a drop around 17 K as SEY starts to decrease from 3.7 reaching 1.3 at 24 K. Differently from the HEPB curve, for the LEPB range the SEY curve shows a clear decrease from 0.7 at 22 K reaching 0.35 at 26 K. Increasing temperature, around 34 K, another slow decrease is visible in the Low-Energy curve and, after this, SEY arrives at 0.15.

It is possible to correlate the SEY variations with different stages in the Ar desorption. The fast scans and low heating rate give the possibility to follow the process, distinguishing the progressive desorption of Ar layers. Taking in account this, the strong and wide variation observed in the HEPB range can be attributed to the progressive desorption of thick Ar multilayer. After desorption of the thick structure, SEY starts to be determined by the Cu substrate and no other changes are visible at higher temperature. In the LEPB range, SEY is not directly influenced by desorption of the Ar thick

film, as observed in the adsorption process, and remains constant during desorption of multilayer. When the layers on the surface are few enough, the primary electrons interact also with substrate. Then the observed variation can be presumably correlated to desorption of these few layers from copper surface. After complete Ar desorption, at 33 K the SEY curve presents the same value observed before adsorption. This value is higher than that observed for clean copper at room temperature as it has been discussed above. The variation of SEY observed between 33 and 40 K can be attributed to the desorption of sub monolayer contaminants absorbed during initial sample cooling down, as it has been discussed above.

The comparing of these preliminary results with literature reveals that the Ar monolayer and multilayer desorption present a shift of about 15 K towards low temperature. A possible explanation to this shift might be found in desorption induced by the interaction between electron beam and Ar film, as observed in other measurements not reported here. In this contest, more data are under study. In this respect, we would like to point out that the aim of these preliminary results is to show the powerfulness and the capability of the SEY technique to study desorption processes, in particular in the LEPB range.

3.2. CARBON MONOXIDE ICES

Figure 8a shows the SEY curves measured on the clean polycrystalline Cu sample during the adsorption of carbon monoxide (CO) at 10 K. The CO/Cu sample presents a behaviour completely different from Ar/Cu.

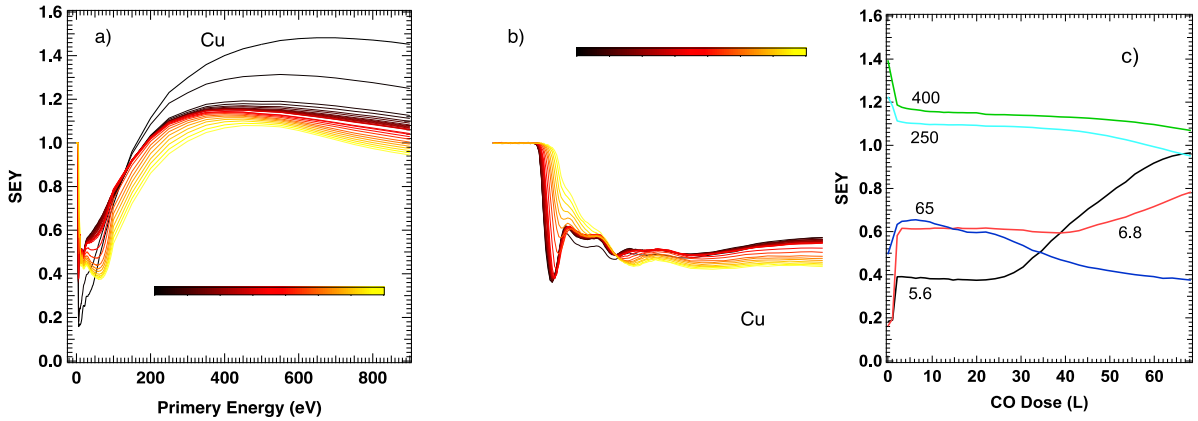

Figure 8: SEY curves versus primary electrons energy as a function of the CO dose in the a) 0 and 900 eV and b) 0 and 30 eV ranges; c) SEY trend at specific energy versus CO dose.

Starting from clean Cu (top black curve in Figure 8a) a low dose of CO (<25 L) determines a decrease of the whole SEY curve. Its maximum becomes 1.16 at 350 eV. With additional exposure to CO the SEY curve changes progressively and at 70 L its maximum is 1.08 at 450 eV.

Figure 8b shows that in the LEPB range, adsorption of CO determines the appearance of different peaks, in particular at 5.6, 6.8, 12.8 and 15 eV. For two of them (5.6 and 6.8 eV) the behaviours exhibited as a function of the CO dose and reported in Figure 8c, show a fast rise at low CO coverage (1-3 L), constant values up to 25-40 L and slow but continuous increase for higher CO dose.

As observed with Ar, also with CO there are different trends at different coverages. The first one is represented by the adsorption of few CO molecules on the substrate, dosing few Langmuir; this process is well recognizable with the first strong variation in SEY curves in the HEPB and LEPB range and with the new characteristic features in LEPB range. As described above, the strong variation in the low energy range might be attributed to a variation in the total reflectivity of the system. Furthermore, the SEY curves show a line shapes much more structured then in the case of Ar/Cu probably due to the more complex interaction of the CO molecules with the Cu substrate. After this, the behaviour between 5 and 25 L, with no significant SEY variation, can be attributed to the gradual formation of a complete layer, or few layers, of CO on the copper surface. At these coverages, the contribution of the substrate to secondary emission is always predominant, but SEY is modified by the presence of CO molecules.

At CO dose above 30 L, the formation of a thicker CO layer determines strong SEY variations mainly in the very low energy range and around 65 eV, and the system follows, at high energy, the trend observed in literature [1]. All these modifications suggest the complexity of the system and in order to take obtain a better and complete comprehension of the adsorption process, more detailed studies are foreseen.

3.3. ELECTRON BEAM INTERACTION

In order to have a better comprehension of the possible interaction between primary beam and Ar ice, another adsorption experiment was performed. After reaching an Ar multi layer configuration with a maximum SEY of 2.6 at 930 eV, equivalent to 12 L, the sample was kept under continuous measuring scans. The result is shown in Figure 9. In the right panel is reported the SEY behaviour at two different energies, 10 and 930 eV. It is possible to observe how, after each scan, the SEY decreases as a function of time, going towards a SEY value of 1.5.

Indeed, the electron gun itself induce non-thermal desorption which needs to be studied in details. If it is true that the desorbed gas is not too high after each scan, so that measuring SEY in a very careful manner and with fast scans of less than a minute in duration, does not affect significantly the ice thickness formed on the surface, it is also true that SEY seems to be the ideal technique to study non-thermal desorption. SEY has been shown to be directly dependent on the amount of cryosorbed gas, and indeed it is achieved by dosing electrons on the surface, which is what will actually happen in the machine during its operation. Of course, all this preliminary consideration has been done as a function of time when repeated scans were performed, which now requires converting this time in actual electron doses. Preliminary cross checks show that the observed behaviour does depend on the electron beam current set, confirming the interest in addressing this issue much more in detail.

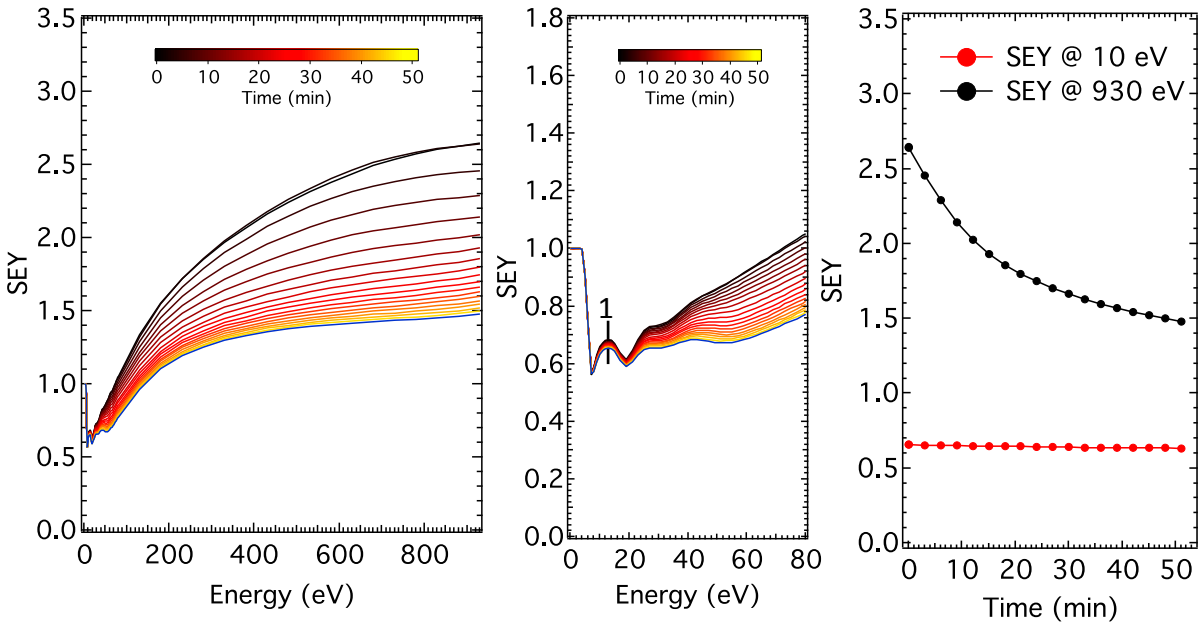

Figure 9: SEY curves versus primary electrons energy as a function of the electron dose in the a) 0 and 900 eV and b) 0 and 30 eV ranges; c) SEY trend at specific energy versus time (electron dose).

4. NEXT STEPS

Before measuring the samples of interest to the collaboration, we intend to continue preliminary studies by studying different gasses (Methane, etc.) and quantifying as carefully as possible the scientific reach that will be available from the use of our set-ups. For this purpose, INFN is funding a significant upgrade of the systems in use, by equipping the XPS system with a specially designed low temperature manipulator. This will allow us to follow with XPS the chemistry occurring at low temperature films, qualifying the actual atomic species and chemical bonds with the very powerful use of XPS spectrometry.

Also, we will add two state-of–the-art “Hiden” quadrupoles for high quality mass spectrometry and we will implement TPD (Temperature Programmed Desorption) on both systems that we intend to continue using. Synchrotron radiation photons, when available, will be an extra feature bursting the activity of our laboratory in view of the final study on vacuum stability objective of this task.

All this equipment, once fully calibrated by the presented measurement and future ones, will be used to fully characterise samples with a variety of different surface treatments and materials in order to determine the best choice for the beam screen inner surface of the FCC-hh cryogenic vacuum chamber.

5. CONCLUSIONS

We showed that our systems and techniques can give unique information on vacuum stability at cryogenic temperature especially in presence of concomitant electron-irradiation of the sample under study. For this purpose, the ongoing upgrade of the experimental stations and the future availability of synchrotron radiation photons, will burst the activity of our laboratory in view of the final study on vacuum stability objective of this task.

6. REFERENCES

[1] A. Kuzucan, H. Neupert, M. Taborelli, H. Stori, "Secondary Electron Yield on cryogenic surfaces as a function of physisorbed gases", J. Vac. Sci. Technol. A 30, pp. 051401, 2012.

[2] R. Cimino, T, Demma, "Electron cloud in accelerators", Int. J. Mod. Phys. A 29, 1430023, July 2014

[3] R. Cimino, I. R. Collins, M. A. Furman, M. Pivi, F. Ruggiero, G. Rumolo, F. Zimmermann, "Can Low-Energy Electrons Affect High-Energy Physics Accelerators?", Phys. Rev. Lett. 93, pp. 014801, July 2004.

[4] R. Cimino and I. R. Collins "Vacuum chamber surface electronic properties influencing electron cloud phenomena" Applied Surface Science 235, 231-235, (2004).

[5] R. Cimino "Surface related properties as an essential ingredient to e-cloud simulations", Nuclear Instruments and Methods in Physics Research A 561, pp. 272–275, 2006

[6] R. Cimino, L. A. Gonzalez, R. Larciprete, A. Di Gaspare, G. Iadarola, G. Rumolo, "Detailed investigation of the low energy secondary electron yield of technical Cu and its relevance for the LHC", Phys. Rev. Special Topics - Accelerators and Beams 18, pp. 051002, 2015.

[7] R. Larciprete, D. R. Grosso, A. Di Trolio, R. Cimino, "Evolution of the secondary electron emission during the graphitization of thin C films", Applied Surface Science 328, pp. 356-360, 2015.

[8] R. Cimino, M. Commisso, D. Grosso, T. Demma, V. Baglin, R. Flammini, R. Larciprete, "Nature of the Decrease of the Secondary-Electron Yield by Electron Bombardment and its Energy Dependence" Phys. Rev. Lett. 109 (2012) 064801.

[9] L. Larciprete, D. R. Grosso, M. Commisso, R. Flamini, R. Cimino, "Secondary electron yield of Cu technical surfaces: Dependence on electron irradiation", Phys. Rev. Special Topics - Accelerators and Beams 16, pp. 011002, 2013.

[10] D.R. Grosso, R. Larciprete, M. Commisso, R. Flammini, R. Cimino and R. Wanzenberg "Effect of the surface processing on the secondary electron yield of Al samples" Phys. Rev. ST Accel. Beams 16, 051003 (2013).

[11] J. Cazaux, Y. Bozhko, N. Hillert, "Electron-induced secondary electron emission yield from condensed rare gases: Ne, Ar, Kr, and Xe", Phys. Rev. B 71, 035419, 2005.

7. ANNEX GLOSSARY

SI units and formatting according to standard ISO 80000-1 on quantities and units are used throughout this document where applicable.

ARUPS	Angular Resolved Ultraviolet Photoemission Spectroscopy.
BS	Beam Screen
FCC	Future Circular Collider
HEPB	High-landing Energy of the Primary Beam
FCC-hh	Hadron Collider within the Future Circular Collider study
HTc	High Critical Temperature
HL-LHC	High Luminosity – Large Hadron Collider
LHC	Large Hadron Collider
LEPB	Low-landing Energy of the Primary Beam
SR	Synchrotron Radiation
SEY	Secondary Electron Emission
TPD	Temperature Programmed Desorbtion
UHV	Ultra-High Vacuum
XPS	X-Ray Photoelectron Spectroscopy
RT	Room Temperature
LT	Low Temperature
LEED	Low Energy Electron Diffraction